Shedding Light on (Anti-)nuclei Production with Pion-Nucleus Femtoscopy

Li-Yuan Zhang, 1,2 Che Ming Ko, 3,* Yu-Gang Ma, 1,2,† Qi-Ye Shou, 1,2,‡ Kai-Jia Sun, 1,2,§ Rui Wang, 4,¶ and Song Zhang 1,2,**

1 Key Laboratory of Nuclear Physics and Ion-beam Application (MOE),

Institute of Modern Physics, Fudan University, Shanghai 200433, China

2 Shanghai Research Center for Theoretical Nuclear Physics,

NSFC and Fudan University, Shanghai 200438, China

3 Cyclotron Institute and Department of Physics and Astronomy,

Texas A&M University, College Station, Texas 77843, USA

4 Istituto Nazionale di Fisica Nucleare (INFN), Sezione di Catania, I-95123 Catania, Italy

High-energy nuclear collisions provide a unique environment for synthesizing both nuclei and antinuclei (such as \bar{d} and $\overline{^4\mathrm{He}}$) at temperatures ($k_BT\sim 100~\mathrm{MeV}$) nearly two orders of magnitude above their binding energies of a few MeV. The underlying production mechanism, whether through statistical hadronization, nucleon coalescence, or dynamical regeneration and disintegration, remains unsettled. By solving relativistic kinetic equations for pion-catalyzed reactions for deuteron regeneration and disintegration ($\pi NN \leftrightarrow \pi d$) in pp collisions at $\sqrt{s}=13~\mathrm{TeV}$, we find pronounced peaks in the femtoscopic momentum correlations of both π^+-p and π^+-d pairs. These peak structures originate from the formation of intermediate Δ (1232) resonances, and their magnitudes agree with recent ALICE measurements when a downward in-medium Δ mass shift of about 70 MeV/ c^2 is included. In contrast, the nucleon coalescence model reproduces only about half of the observed peak strength, and the statistical hadronization model predicts no resonance feature. These findings from pion-nucleus femtoscopy provide compelling evidence that pion-catalyzed reactions play a dominant role in the production of light (anti-)nuclei in high-energy nuclear collisions and cosmic rays.

(Dated: November 14, 2025)

Introduction.— Loosely-bound light nuclei and antinuclei have been measured in high-energy nuclear collisions at Relativistic Heavy Ion Collider (RHIC) and the Large Hadron Collider (LHC) [1–4]. This phenomenon, known as 'little-bang' nucleosynthesis, has attracted renewed interest because of its relevance to matter–antimatter asymmetry tests [5], quarkgluon plasma (QGP) bulk properties [6], and indirect dark matter searches [7, 8]. Despite decades of study, the microscopic mechanism by which such fragile (anti-)nuclei form and survive the hot and dense hadronic environment remains unresolved [9–15].

Three major competing scenarios (see Figure 1) have been proposed, including statistical hadronization model (SHM) [16], nucleon coalescence at kinetic freeze-out [17, 18], and continuous disintegration and regeneration driven by pion-catalyzed reactions in the hadronic phase (e.g. $\pi NN \leftrightarrow \pi d$, $\pi Nd \leftrightarrow \pi^3$ He) [19, 20]. Bulk observables such as yields, p_T spectra, and collective flow [21–25] alone cannot unambiguously distinguish these scenarios, as different models can reproduce similar integrated yields and flow patterns [19, 26].

In contrast, correlation femtoscopy [27, 28] or Hanbury-Brown and Twiss (HBT) interferometry [29–31] has evolved from its origins in astronomical intensity interferometry into a precision tool for probing the spatio-temporal structure of relativistic nuclear collisions. By measuring femtoscopic momentum correlations, one can resolve spatial scales of order 10^{-15} m and temporal scales of order 10^{-23} s [32], and even extract information about the strong interaction in few-body systems [33–35]. Correlation structures can arise from quantum statistics [36], final-state strong and Coulomb interactions [36, 37], or resonance decays [37]. For pion-catalyzed channels such as $\pi^+ np \to \pi^+ d$, the reaction rate peaks through formation of an intermediate $\Delta(1232)$ resonance [20]. This

would produce a characteristic resonant enhancement in the pion-deuteron $(\pi-d)$ correlation function. Such a resonance structure has recently been observed by the ALICE Collaboration [38, 39], though its microscopic origin remains to be clarified.

In the present study, we elucidate the ALICE measurements [38, 39] by solving relativistic kinetic equations for pion-catalyzed regeneration and breakup of (anti-)deuterons in pp collisions at $\sqrt{s} = 13$ TeV and calculating pion-nucleus correlation functions. The resulting $\pi^+ - p$ and $\pi^+ - d$ correlation functions exhibit pronounced resonance peaks at $k^* \simeq$ 0.2 GeV/c, corresponding to Δ excitation. From the comparison with ALICE data, we further reveal an in-medium Δ mass reduction of roughly 70 MeV/ c^2 . Although the coalescence model reproduces similar qualitative trends, it explains only half of the observed peak magnitude, while the statistical hadronization model does not predict any resonance feature. These results demonstrate the unique discriminating power of pion-nucleus femtoscopy and identify pion-catalyzed reactions as the dominant mechanism for the production of light (anti-)nuclei in high-energy nuclear collisions.

Theoretical Framework.— We employ a multi-phase transport (AMPT) model [40] to describe the evolution of the partonic phase created in pp collisions, with hadronization implemented via a quark coalescence mechanism. For the subsequent hadronic evolution and light (anti-)nuclei production, we include not only pion-catalyzed deuteron formation and dissociation but also other relevant scattering channels available in AMPT. These processes describe properly the dynamics of pions and nucleons that are essential for investigating light (anti-)nuclei production.

The effect of $\pi^+ d \leftrightarrow \pi^+ np$ on deuteron production and dissociation in nuclear collisions can be described by the rela-

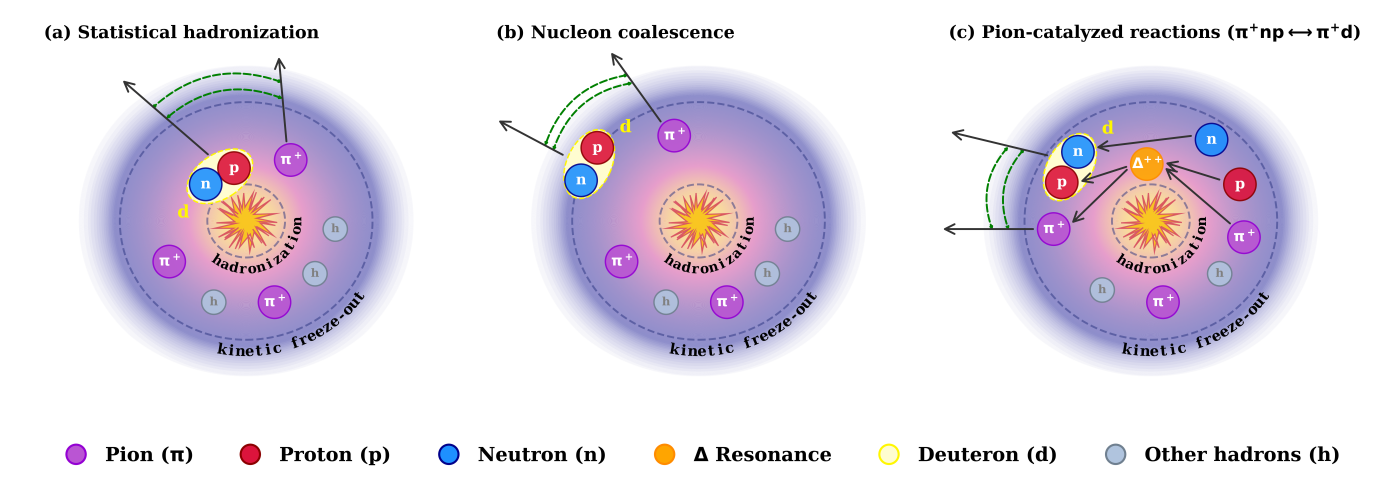


FIG. 1. Scenarios of deuteron production in high-energy nuclear collisions, including the statistical hadronization of QGP (a), the nucleon coalescence at the kinetic freeze-out (b), and the pion-catalyzed reactions (e.g. $\pi^+ np \leftrightarrow \pi^+ d$) with the assistance of intermediate Δ resonance during the hadronic matter expansion (c).

tivistic kinetic equation [20],

$$\frac{\partial f_d}{\partial t} + \frac{\mathbf{P}}{E_d} \cdot \frac{\partial f_d}{\partial \mathbf{R}} = -\mathcal{K}^{>} f_d + \mathcal{K}^{<} (1 + f_d), \tag{1}$$

where $f_d(\mathbf{R}, \mathbf{P})$ denotes the phase space distribution of deuteron, and $\mathcal{K}^>$ and $\mathcal{K}^<$ denote respectively dissociation and regeneration rates with their expressions given in Ref. [20]. The effect of mean field is neglected due to the fact that the particle kinetic energy is much larger than the potential energy.

Eq. (1) has been shown to successfully describe deuteron production in Au+Au and Pb+Pb collisions [19, 20]. It was solved using a stochastic method with test particles [20]. In this method, the probability that the reaction $\pi^+d \to \pi^+np$ occurs between a pion and a deuteron within the volume ΔV during the time interval Δt under the impulse approximation (IA) is given by [20, 41–43]

$$P_{23}|_{\mathrm{IA}} \approx F_d v_{\pi^+ p} \sigma_{\pi^+ p \to \pi^+ p} \frac{\Delta t}{N_{\mathrm{test}} \Delta V} + (p \leftrightarrow n),$$
 (2)

where v_{π^+p} denotes the relative speed between the pion and the proton within the deuteron, and N_{test} refers to the number of test particles [44]. The pion-nucleon cross section is given by $\sigma(E) = 2\pi g \tilde{\Gamma} \mathcal{A}(E)/q_0^2$ where $\mathcal{A}(E)$ describes the spectral shape of the Δ resonance using the Sill distribution [39, 45],

$$\mathcal{A}(E) = \frac{2E}{\pi} \frac{\sqrt{E^2 - E_{\text{th}}^2} \tilde{\Gamma}}{(E^2 - m_{\Delta}^2)^2 + (E^2 - E_{\text{th}}^2) \tilde{\Gamma}^2} \Theta(E - E_{\text{th}}), (3)$$

The rescaled width is defined as $\tilde{\Gamma} = \Gamma_{\Delta} m_{\Delta} / \sqrt{m_{\Delta}^2 - E_{\rm th}^2}$ with $E_{\rm th}$ being the threshold energy $E_{\rm th} = m_{\pi} + m_p$. For all four isospin states of Δ , we take their width as $\Gamma_{\Delta} = 0.117$ GeV and their mass as $m_{\Delta} = 1.232$ (GeV/ c^2) + δm_{Δ} where δm_{Δ} is introduced as an in-medium mass shift and it vanishes in

vacuum. For $\pi^+ - p$ scattering, the statistical spin factor is g=2 and the reference momentum is taken as $q_0=0.18$ GeV/c to reproduce the experimental data on $\pi^+ - p$ cross section. Employing a constant value of $F_d \approx 0.72$ yields an accurate description of the measured $\pi + d$ dissociation cross sections [46] within the energy domain relevant to the present study.

A sufficiently large $N_{\rm test}$ is typically required for the convergence of numerical results. However, calculating femtoscopic correlation functions necessitates event-by-event simulations, which corresponds to $N_{\rm test}=1$. This is because correlations are smeared out for $N_{\rm test}>1$. To overcome this limitation, we replace the $1/\Delta V$ factor in Eqs. (2) and (5) with a Gaussian smearing function, $S_{ij}=e^{-d_{ij}^2/(2l^2)}/(2\pi l^2)^{\frac{3}{2}}$, where d_{ij} is the spatial distance between particles i and j, and l denotes the effective interaction range. This treatment mimics the scattering of two Gaussian wave packets [14]. With this modification, Eq. (2) is rewritten as

$$P_{23}|_{\mathrm{IA}} \approx F_d v_{\pi^+ p} \sigma_{\pi^+ p \to \pi^+ p} S_{\pi^+ p} \Delta t + (p \leftrightarrow n).$$
 (4)

The choice of l does not affect the momentum correlations of the outgoing particles and it is set as l = 1.2 fm in the following calculation.

Similarly, the probability for the reaction $\pi^+ np \to \pi^+ d$ to take place in a time interval Δt is

$$P_{32}|_{\mathrm{IA}} \approx \frac{3}{4} F_d v_{\pi^+ p} \sigma_{\pi^+ p \to \pi^+ p} S_{\pi^+ p} W_d \Delta t + (p \leftrightarrow n), \qquad (5)$$

where W_d stands for the deuteron Wigner function, characterizing the nonlocal features of the scattering as it depends simultaneously on the positions and momenta of the constituent nucleons inside the deuteron.

With the obtained particle phase-space information at the kinetic freeze-out (defined as the phase-space positions at last

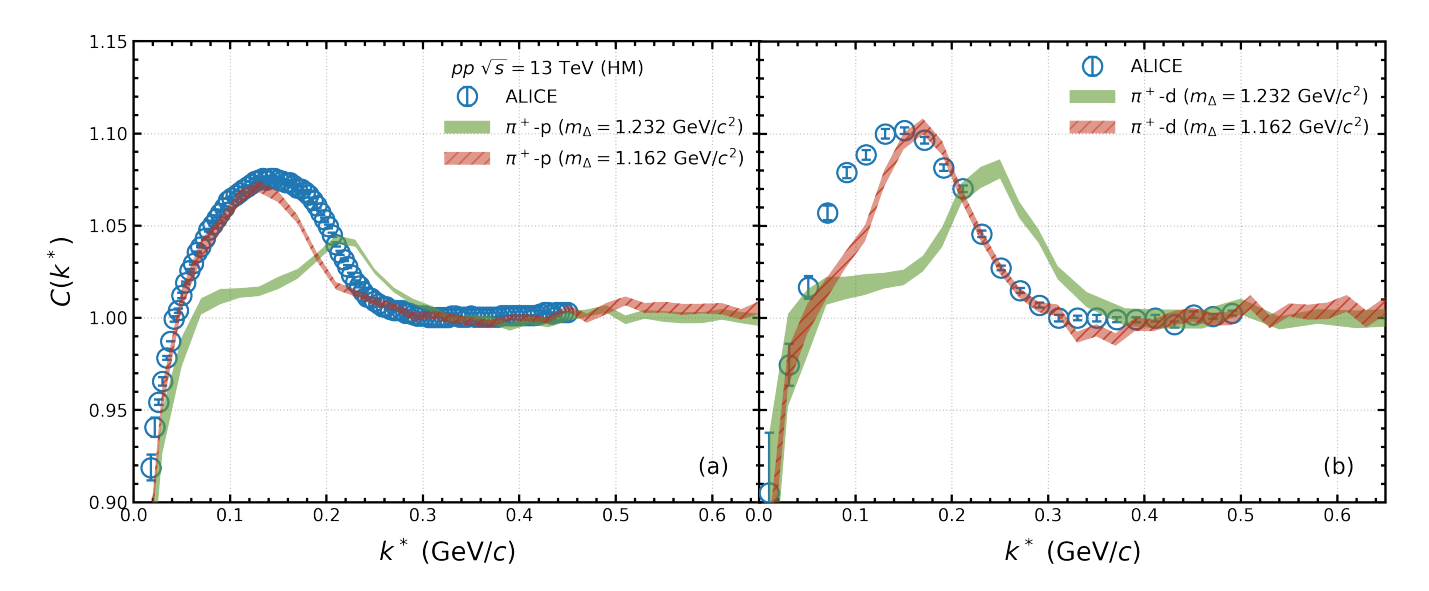


FIG. 2. Correlation function $C(k^*)$ of $\pi^+ - p$ (a) and $\pi^+ - d$ (b) in high-multiplicity pp collisions at $\sqrt{s} = 13$ TeV. Theoretical results with nominal and reduced Δ masses are shown by green and purple (red) bands, respectively. Experimental data with combined statistical and systematic uncertainties taken from the ALICE Collaboration [38, 39] are denoted by filled symbols. Following the experimental kinematic cuts, particle rapidity is restricted to $|\eta| \le 0.8$. The transverse momentum (p_T) is required to be within the range $0.14 < p_T < 4.0$ GeV/c for pions and $0.5 < p_T < 2.4$ GeV/c for deuterons. For $\pi^+ - p$ correlations, additional cut of pair transverse momentum, defined by $m_T = \sqrt{(m_P + m_\pi)^2 + (\mathbf{k}_P + \mathbf{k}_\pi)^2}/2$, of $m_T \in [0.54 \ 0.75)$ GeV/c² is imposed [38].

collisions), the two-particle correlation function is then given by [28, 47]

$$C(\mathbf{k}^*) = \mathcal{N} \frac{\sum_{\text{pairs}}^{\text{same}} \delta(\mathbf{k}_{\text{pair}}^* - \mathbf{k}^*) |\Psi_{\mathbf{k}^*}(\mathbf{r}^*)|^2}{\sum_{\text{pairs}}^{\text{mixed}} \delta(\mathbf{k}_{\text{pair}}^* - \mathbf{k}^*)},$$
(6)

where $\mathbf{r}^* = \mathbf{r}_2 - \mathbf{r}_1$ is the relative spatial separation of the two particles after the earlier freeze-out particle is freely propagated to the time when the later one freezes out, $\mathbf{k}^* = (\mathbf{k}_2^* (\mathbf{k}_1^*)/2$ is the reduced relative momentum in the pair rest frame (PRF), and $\Psi_{\mathbf{k}^*}(\mathbf{r}^*)$ is the Bethe-Salpeter (BS) amplitude responsible for the final-state interactions (FSI). In the region of interest with small k^* , the short-range particle interaction is dominated by the s-wave interaction, and the asymptotic solution of the wave function of the two charged particles is given in Refs. [32, 48]. The numerator represents the distribution of relative momenta between two particles emitted within the same collision event. Conversely, the denominator corresponds to the mixed-event distribution that serves as a reference that reflects the underlying phase space without the influence of FSI. Due to the small scattering parameters of the pion-nucleus pair, e.g., the scattering length of $\pi^+ - d(p)$ pair is about -0.037 (-0.13) fm [49, 50], the strong interaction contribution is thus small. The factor \mathcal{N} in Eq. (6) denotes the normalizing constant ensuring that $C(k^*)$ is unity at large k^* where momentum correlation becomes negligible.

Pion-nucleus femtoscopy in pp collisions at $\sqrt{s} = 13$ TeV.— We now compute the pion-nucleus femtoscopic correlation functions in high-multiplicity (HM) [51] pp collisions at $\sqrt{s} = 13$ TeV using Eq. (6). Figure 2 displays the

correlation functions $C(k^*)$ for the pairs (a) $\pi^+ - p$ and (b) $\pi^+ - d$ from theoretical calculations as well as their comparison with experimental data from the ALICE Collaboration [38, 39], which are denoted by filled symbols together with their combined statistical and systematic uncertainties. Theoretical results using nominal Δ mass $m_{\Delta} = 1.232 \text{ GeV}/c^2$ are represented by green bands (with charged particle multiplicity $\langle dN_{\rm ch}/d\eta \rangle \approx 26$) and display pronounced peaks at $k^* \approx 0.22 \text{ GeV}/c$. At the very low relative momentum $k^* \leq 0.05 \text{ GeV}/c$, correlation functions are suppressed by the repulsive Coulomb force between $\pi^+ - p$ and $\pi^+ - d$ pairs.

For the π^+ – p correlation, the peak originates from the decay $\Delta^{++} \to \pi^+ + p$. In the case of $\pi^+ - d$ correlations, the peaks originate from forward pion-catalyzed reactions $\pi NN \rightarrow \pi d$ whose rates are the largest in the excitation region of intermediate Δ resonances [20]. Alternatively, in the Δ -dominated region one may view these as sequential Δ -assisted processes, $\pi N \leftrightarrow \Delta$ and $\Delta N \leftrightarrow \pi d$. In both correlation functions, the ALICE data reveal pronounced peaks at a lower relative momentum of $k^* \approx 0.15 \text{ GeV}/c$. This downward shift was initially interpreted as a very low spectrum temperature $k_BT \approx 20\text{--}30 \text{ MeV}$ [38, 39], far below the typical kinetic freeze-out temperature usually higher than 100 MeV in pp collisions [52]. A more plausible explanation for the observed Δ peak mass shift in pp collisions is its in-medium modification through interactions with the hot hadronic environment [53] or through partial restoration of chiral symmetry [54, 55]. In particular, thermal QCD sum-rule calculations predict a Δ mass reduction of approximately 70 MeV at a temperature of T = 150 MeV [55].

Similar shifts in the Δ mass have been observed previously in minimum-bias pp and d+Au collisions at $\sqrt{s_{NN}} = 200$ GeV [56], in Au+Au collisions at $\sqrt{s_{NN}} = 2.4$ GeV [57], and in earlier fixed-target experiments [58, 59]. At low collision energies ($\sqrt{s_{NN}} < 3$ GeV), these mass modifications were attributed to effects such as Δ regeneration near the kinetic freeze-out stage [60, 61] and thermalization with cold nuclear matter [58, 62].

To phenomenologically account for this shift, we reduce the Δ mass in our model from 1.232 to 1.162 GeV by setting $\delta m_{\Delta} = -70$ MeV. The resulting $\pi^+ - p$ correlation function, shown as red bands in Fig. 2, now peaks at $k \approx 0.15 \,\text{GeV}/c$, in much better agreement with the data. A similar mass shift is also observed in the π^+ – d correlation, where the peak moves from $k \approx 0.22$ to 0.17 GeV/c. The model reproduces the experimental data well for $k^* > 0.15 \text{ GeV}/c$, but underestimates the correlation strength for lower k^* at 0.05 - 0.15 GeV/c. Further reducing the in-medium Δ mass improves the description of the π^+ – d correlation but simultaneously worsens the agreement with the π^+ – p correlation. Improved agreements may be achieved in the future by extending the present kinetic approach to include off-shell effects of pions and nucleons within the S-matrix formalism [63] or the chiral effective field theory [64].

Pion-nucleus femtoscopy in different production scenarios.— We next investigate the pion–nucleus correlation functions within two alternative frameworks: the nucleon coalescence model [17, 65] and the statistical hadronization model [16]. In the coalescence approach, deuterons form via $n + p \rightarrow d$ at the kinetic freeze-out, and its number (N_d) is given by [17]

$$N_d = \sum_{np} g_d W_d = \sum_{np} 6 \exp\left(-\frac{\rho^2}{\sigma_d^2} - \sigma_d^2 k_\rho^2\right), \tag{7}$$

where the summation is over all pairs of neutron and proton in each collision event, $g_d = 3/4$ is the statistical factor for forming a deuteron of spin 1 from two spin 1/2 proton and neutron, the deuteron Wigner function W_d is taken to be Gaussian in spatial and momentum coordinates for simplicity. The Jacobi coordinates and momenta are defined by $\rho = \mathbf{r}_2 - \mathbf{r}_1$, $k_\rho = (\mathbf{k}_2 - \mathbf{k}_1)/2$ where \mathbf{r}_1 and \mathbf{r}_2 are the spatial coordinates of neutron, and proton, respectively, at an equal time in their rest frame, and they are determined by propagating the constituent nucleons of momenta \mathbf{k}_1 and \mathbf{k}_2 at earlier freeze-out times to the time of the later freeze-out one. The width parameter is taken as $\sigma_d = \sqrt{8/3} \, r_d \approx 3.2$ fm to reproduce the deuteron size [66, 67].

The resulting π^+ –d correlation function from the coalescence model is shown by the purple band in Fig. 3. A residual correlation appears when one of the nucleons participating in $n+p \to d$ originates from the Δ decay, since the deuteron inherits the π –N correlation from its constituent. Conversely, if neither nucleon originates from a Δ , no such correlation remains. Consequently, the coalescence-induced peak is significantly weaker than that generated by pion-catalyzed reactions—less than half the strength observed in both the ALICE

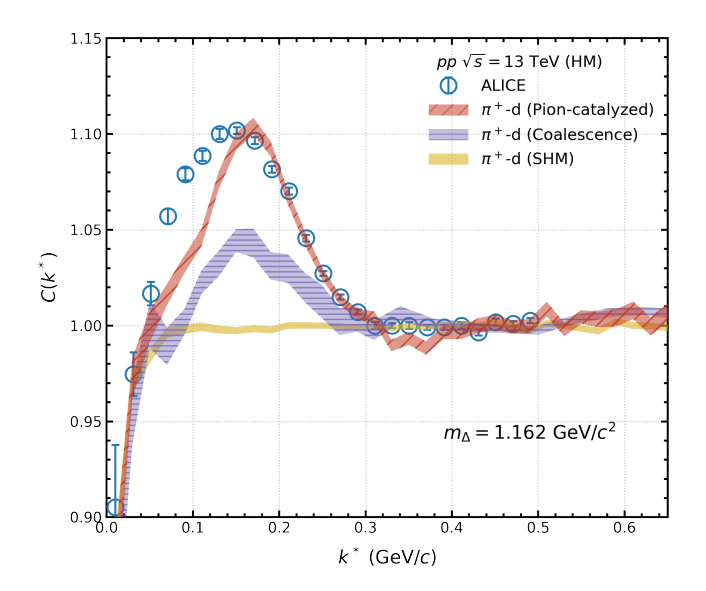


FIG. 3. Correlation function $C(k^*)$ of $\pi^+ - d$ in different production scenarios for pp collisions at $\sqrt{s} = 13$ TeV. Experimental data shown as filled symbols are taken from the ALICE Collaboration [39], and theoretical predictions are represented by colored bands.

data and the pion-catalysis calculations (red band in Fig. 3).

In the statistical hadronization approach, pions and light nuclei are emitted independently from a thermalized expanding source, described here by a blast-wave parameterization using the parameters from Ref. [39]. After including the Coulomb interaction between the pion and deuteron, the calculated $\pi^+ - d$ correlation function, shown by the yellow band in Fig. 3, exhibits the expected low- k^* suppression due to repulsion but lacks any resonance-like structure associated with Δ formation, consistent with results reported in Ref. [39].

The comparison in Fig. 3 demonstrates that the pioncatalyzed reaction framework provides the most accurate description of the ALICE data. The clearly distinct predictions of the three approaches highlight the strong discriminating power of pion–nucleus femtoscopy as a sensitive probe of the underlying dynamics of (anti-)nuclei production.

Conclusion.—In the present study, we have elucidated the production mechanism of light nuclei in high-energy nuclear collisions by employing the novel method of pion–nucleus femtoscopy, which enables clear differentiation among competing formation scenarios.

By solving relativistic kinetic equations for pion-catalyzed reactions $(\pi NN \leftrightarrow \pi d)$ on an event-by-event basis, we obtain femtoscopic momentum correlations of $\pi^+ - p$ and $\pi^+ - d$ pairs in high-multiplicity pp collisions at $\sqrt{s} = 13$ TeV. Both correlation functions show pronounced peaks associated with the excitation of the $\Delta(1232)$ resonance. A comparison with the ALICE data reveals a downward mass shift of the Δ resonance by about 70 MeV/ c^2 , indicating strong in-medium effects. While the nucleon coalescence model reproduces qualitatively similar features, the peak magnitude is only about

half of that observed, and the statistical hadronization model predicts no resonance structure. Among the three scenarios considered (see Fig. 1), the pion-catalyzed reaction framework provides the most accurate and consistent description of the ALICE measurements (see Fig. 3), offering compelling evidence that pion-catalyzed reactions dominate light (anti-)nuclei production at LHC energies.

The present framework can be readily extended to larger collision systems such p+Pb, O+O, Ru+Ru, Zr+Zr, Au+Au, and Pb+Pb, spanning beam energies from a few GeV to several TeV. Further exploration of femtoscopic correlations involving heavier light nuclei, such as pion-helium (π – 3 He), pion-triton (π – 3 H), pion-alpha (π – 4 He), and pion-hypertriton (π – 3 H) pairs, will provide deeper insight into the production dynamics of (anti-)(hyper-)nuclei in high-energy collisions and cosmic rays.

Acknowledgments.— We thank Lie-Wen Chen, Mei-Yi Chen, Bhawani Singh, Laura Fabbietti, Yi-Heng Feng, Feng-Kun Guo, Dimitar Mihaylov, Pok Man Lo, Xiao-Feng Luo, Dong-Fang Wang, and Zhen Zhang for fruitful discussions. This work was supported in part by the National Key Research and Development Project of China under Grant No. 2024YFA1612500, the National Natural Science Foundation of China under Contracts No. 12422509, No. 12375121, 12025501, No. 12147101, No. 11891070, No. 124B2102, No. 12275054, No. 12061141008, Shanghai Pilot Program for Basic Research - Fudan University 21TQ1400100(22TQ006), the Guangdong Major Project of Basic and Applied Basic Research No. 2020B0301030008, and the STCSM under Grant No. 23590780100. The computations in this research were performed using the CFFF platform of Fudan University.

- * ko@comp.tamu.edu
- † Corresponding author: mayugang@fudan.edu.cn
- * shougiye@fudan.edu.cn
- § Corresponding author: kjsun@fudan.edu.cn
- ¶ rui.wang@lns.infn.it
- ** Corresponding author: song_zhang@fudan.edu.cn
- [1] B. I. Abelev *et al.* (STAR), Observation of an Antimatter Hypernucleus, Science **328**, 58 (2010).
- [2] H. Agakishiev *et al.* (STAR), Observation of the antimatter helium-4 nucleus, Nature 473, 353 (2011), [Erratum: Nature 475, 412 (2011)].
- [3] M. Abdulhamid *et al.* (STAR), Observation of the antimatter hypernucleus ⁴H̄, Nature 632, 1026 (2024).
- [4] S. Acharya *et al.* (ALICE), First Measurement of A = 4 Hypernuclei and Antihypernuclei at the LHC, Phys. Rev. Lett. 134, 162301 (2025).
- [5] ALICE Collaboration, Precision measurement of the mass difference between light nuclei and anti-nuclei, Nature Phys. 11, 811 (2015).
- [6] D. Everett *et al.* (JETSCAPE), Role of bulk viscosity in deuteron production in ultrarelativistic nuclear collisions, Phys. Rev. C 106, 064901 (2022).
- [7] P. von Doetinchem et. al, Cosmic-ray antinuclei as messengers

- of new physics: status and outlook for the new decade, J. Cosmol. Astropart. Phys. **08**, 035.
- [8] S. Acharya et al. (ALICE), Measurement of anti-³He nuclei absorption in matter and impact on their propagation in the Galaxy, Nature Phys. 19, 61 (2023).
- [9] S. T. Butler and C. A. Pearson, Deuterons from High-Energy Proton Bombardment of Matter, Phys. Rev. 129, 836 (1963).
- [10] J. I. Kapusta, Mechanisms for deuteron production in relativistic nuclear collisions, Phys. Rev. C 21, 1301 (1980).
- [11] L. P. Csernai and J. I. Kapusta, Entropy and Cluster Production in Nuclear Collisions, Phys. Rept. 131, 223 (1986).
- [12] P. Braun-Munzinger and B. Dönigus, Loosely-bound objects produced in nuclear collisions at the LHC, Nucl. Phys. A 987, 144 (2019).
- [13] J. Chen, D. Keane, Y.-G. Ma, A. Tang, and Z. Xu, Antinuclei in Heavy-Ion Collisions, Phys. Rept. 760, 1 (2018).
- [14] A. Ono, Dynamics of clusters and fragments in heavy-ion collisions, Prog. Part. Nucl. Phys. 105, 139 (2019).
- [15] E. Braaten, K. Ingles, and J. Pickett, Explaining Snowball-in-Hell Phenomena in Heavy-Ion Collisions Using a Novel Thermodynamic Variable, Phys. Rev. Lett. 134, 252301 (2025).
- [16] A. Andronic, P. Braun-Munzinger, K. Redlich, and J. Stachel, Decoding the phase structure of QCD via particle production at high energy, Nature 561, 321 (2018).
- [17] R. Scheibl and U. Heinz, Coalescence and flow in ultrarelativistic heavy ion collisions, Phys. Rev. C 59, 1585 (1999).
- [18] F. Bellini, K. Blum, A. P. Kalweit, and M. Puccio, Examination of coalescence as the origin of nuclei in hadronic collisions, Phys. Rev. C 103, 014907 (2021).
- [19] D. Oliinychenko, L.-G. Pang, H. Elfner, and V. Koch (SMASH), Microscopic study of deuteron production in PbPb collisions at $\sqrt{s} = 2.76 TeV$ via hydrodynamics and a hadronic afterburner, Phys. Rev. C **99**, 044907 (2019).
- [20] K.-J. Sun, R. Wang, C. M. Ko, Y.-G. Ma, and C. Shen, Unveiling the dynamics of little-bang nucleosynthesis, Nature Commun. 15, 1074 (2024).
- [21] S. S. Adler *et al.* (PHENIX), Deuteron and antideuteron production in Au + Au collisions at s(NN)**(1/2) = 200-GeV, Phys. Rev. Lett. **94**, 122302 (2005).
- [22] S. Acharya *et al.* (ALICE), Production of light (anti)nuclei in pp collisions at $\sqrt{s} = 13$ TeV, JHEP **01**, 106.
- [23] S. Acharya *et al.* (ALICE), Enhanced Deuteron Coalescence Probability in Jets, Phys. Rev. Lett. 131, 042301 (2023).
- [24] M. Abdulhamid *et al.* (STAR), Beam Energy Dependence of Triton Production and Yield Ratio $(N_t \times N_p/N_d^2)$ in Au+Au Collisions at RHIC, Phys. Rev. Lett. **130**, 202301 (2023).
- [25] B. Aboona *et al.* (STAR), Observation of Directed Flow of Hypernuclei HΛ3 and HΛ4 in sNN=3 GeV Au+Au Collisions at RHIC, Phys. Rev. Lett. 130, 212301 (2023).
- [26] S. Acharya *et al.* (ALICE), Elliptic and triangular flow of (anti)deuterons in Pb-Pb collisions at $\sqrt{s_{\rm NN}}$ = 5.02 TeV, Phys. Rev. C **102**, 055203 (2020).
- [27] R. Lednicky, Progress in correlation femtoscopy, in 32nd International Symposium on Multiparticle Dynamics (2002) pp. 21–26, arXiv:nucl-th/0212089.
- [28] M. A. Lisa, S. Pratt, R. Soltz, and U. Wiedemann, Femtoscopy in relativistic heavy ion collisions, Ann. Rev. Nucl. Part. Sci. 55, 357 (2005).
- [29] R. Hanbury Brown and R. Q. Twiss, A Test of a new type of stellar interferometer on Sirius, Nature 178, 1046 (1956).
- [30] G. Baym, The Physics of Hanbury Brown-Twiss intensity interferometry: From stars to nuclear collisions, Acta Phys. Polon. B 29, 1839 (1998).
- [31] U. W. Heinz and B. V. Jacak, Two particle correlations in rela-

- tivistic heavy ion collisions, Ann. Rev. Nucl. Part. Sci. 49, 529 (1999).
- [32] R. Lednicky and V. L. Lyuboshits, Final State Interaction Effect on Pairing Correlations Between Particles with Small Relative Momenta, Yad. Fiz. 35, 1316 (1981).
- [33] S. Acharya et al. (ALICE), Scattering studies with low-energy kaon-proton femtoscopy in proton-proton collisions at the LHC, Phys. Rev. Lett. 124, 092301 (2020).
- [34] L. Fabbietti, V. Mantovani Sarti, and O. Vazquez Doce, Study of the Strong Interaction Among Hadrons with Correlations at the LHC, Ann. Rev. Nucl. Part. Sci. 71, 377 (2021).
- [35] D. Si et al., Extracting Neutron-Neutron Interaction Strength and Spatiotemporal Dynamics of Neutron Emission from the Two-Particle Correlation Function, Phys. Rev. Lett. 134, 222301 (2025).
- [36] S. E. Koonin, Proton Pictures of High-Energy Nuclear Collisions, Phys. Lett. B 70, 43 (1977).
- [37] U. A. Wiedemann and U. W. Heinz, Resonance contributions to HBT correlation radii, Phys. Rev. C 56, 3265 (1997).
- [38] S. Acharya *et al.* (ALICE), Investigating the p- π^{\pm} and p-p- π^{\pm} dynamics with femtoscopy in pp collisions at $\sqrt{s} = 13$ TeV, Eur. Phys. J. A **61**, 194 (2025).
- [39] S. Acharya *et al.* (ALICE), Revealing the microscopic mechanism of deuteron formation at the LHC, (2025), arXiv:2504.02393 [nucl-ex].
- [40] Z.-W. Lin, C. M. Ko, B.-A. Li, B. Zhang, and S. Pal, A Multiphase transport model for relativistic heavy ion collisions, Phys. Rev. C 72, 064901 (2005).
- [41] P. Danielewicz and G. F. Bertsch, Production of deuterons and pions in a transport model of energetic heavy ion reactions, Nucl. Phys. A 533, 712 (1991).
- [42] Z. Xu and C. Greiner, Thermalization of gluons in ultrarelativistic heavy ion collisions by including three-body interactions in a parton cascade, Phys. Rev. C 71, 064901 (2005).
- [43] R. Wang, Z. Zhang, L.-W. Chen, and Y.-G. Ma, Nuclear Collective Dynamics in Transport Model With the Lattice Hamiltonian Method, Front. in Phys. 8, 330 (2020).
- [44] C.-Y. Wong, Dynamics of nuclear fluid. VIII. Time-dependent Hartree-Fock approximation from a classical point of view, Phys. Rev. C 25, 1460 (1982).
- [45] F. Giacosa, A. Okopińska, and V. Shastry, A simple alternative to the relativistic Breit–Wigner distribution, Eur. Phys. J. A 57, 336 (2021).
- [46] P. A. Zyla et al. (Particle Data Group), Review of Particle Physics, PTEP 2020, 083C01 (2020).
- [47] A. Kisiel, Non-identical particle femtoscopy at s(NN)**(1/2) = 200-AGeV in hydrodynamics with statistical hadronization, Phys. Rev. C **81**, 064906 (2010).
- [48] R. Lednicky, Finite-size effects on two-particle production in continuous and discrete spectrum, Phys. Part. Nucl. 40, 307 (2009).
- [49] T. E. O. Ericson, B. Loiseau, and A. W. Thomas, Determination of the pion nucleon coupling constant and scattering lengths, Phys. Rev. C 66, 014005 (2002).

- [50] S. R. Beane, V. Bernard, E. Epelbaum, U.-G. Meissner, and D. R. Phillips, The S wave pion nucleon scattering lengths from pionic atoms using effective field theory, Nucl. Phys. A 720, 399 (2003).
- [51] S. Acharya *et al.* (ALICE), Investigation of the p–Σ0 interaction via femtoscopy in pp collisions, Phys. Lett. B 805, 135419 (2020), 1910.14407.
- [52] S. Acharya *et al.* (ALICE), Multiplicity dependence of π , K, and p production in pp collisions at $\sqrt{s} = 13$ TeV, Eur. Phys. J. C **80**, 693 (2020).
- [53] K. Azizi and G. Bozkır, Decuplet baryons in a hot medium, Eur. Phys. J. C 76, 521 (2016).
- [54] J. M. Torres-Rincon, B. Sintes, and J. Aichelin, Flavor dependence of baryon melting temperature in effective models of QCD, Phys. Rev. C 91, 065206 (2015).
- [55] Y.-J. Xu, Y.-L. Liu, and M.-Q. Huang, Temperature Dependence of Decuplet Baryon Masses from Thermal QCD Sum Rules, Commun. Theor. Phys. 63, 209 (2015).
- [56] B. I. Abelev *et al.* (STAR), Hadronic resonance production in d+Au collisions at s(NN)**(1/2) = 200-GeV at RHIC, Phys. Rev. C 78, 044906 (2008).
- [57] J. Adamczewski-Musch *et al.*, Correlated pion-proton pair emission off hot and dense QCD matter, Phys. Lett. B 819, 136421 (2021).
- [58] M. Eskef *et al.* (FOPI), Identification of baryon resonances in central heavy ion collisions at energies between 1-AGeV and 2-AGeV, Eur. Phys. J. A 3, 335 (1998).
- [59] E. L. Hjort et al., Delta resonance production in Ni-58 + Cu collisions at E = 1.97-A-GeV, Phys. Rev. Lett. 79, 4345 (1997).
- [60] T. Reichert, P. Hillmann, A. Limphirat, C. Herold, and M. Bleicher, Delta mass shift as a thermometer of kinetic decoupling in Au + Au reactions at 1.23 AGeV, J. Phys. G 46, 105107 (2019).
- [61] T. Reichert, P. Hillmann, and M. Bleicher, Δ resonances in Ca+Ca, Ni+Ni and Au+Au reactions from 1 AGeV to 2 AGeV: Consistency between yields, mass shifts and decoupling temperatures, Nucl. Phys. A 1007, 122058 (2021).
- [62] W. Weinhold, B. L. Friman, and W. Noerenberg, Thermodynamics of an interacting pi N system, Acta Phys. Polon. B 27, 3249 (1996).
- [63] P. M. Lo, S-matrix formulation of thermodynamics with N-body scatterings, Eur. Phys. J. C 77, 533 (2017).
- [64] V. Baru, J. Haidenbauer, C. Hanhart, A. E. Kudryavtsev, V. Lensky, and U.-G. Meissner, Role of the Delta(1232) in piondeuteron scattering at threshold within chiral effective field theory, Phys. Lett. B 659, 184 (2008).
- [65] K.-J. Sun, C. M. Ko, and B. Dönigus, Suppression of light nuclei production in collisions of small systems at the Large Hadron Collider, Phys. Lett. B 792, 132 (2019).
- [66] K.-J. Sun and L.-W. Chen, Analytical coalescence formula for particle production in relativistic heavy-ion collisions, Phys. Rev. C 95, 044905 (2017).
- [67] G. Ropke, Light nuclei quasiparticle energy shift in hot and dense nuclear matter, Phys. Rev. C 79, 014002 (2009).